International Journal of Astrophysics and Space Science
2023; 11(2): 23-37
http://www.sciencepublishinggroup.com/j/ijass
doi: 10.11648/j.ijass.20231102.12
ISSN: 2376-7014 (Print); ISSN: 2376-7022 (Online)

Protoplanetary Disk Formation in a Self-gravitating Molecular Cloud

Gemechu Muleta Kumssa[1, 2, *], Solomon Belay Tessema[1]

[1]Space Science and Geospatial Institute (SSGI), Entoto Observatory and Research Center (EORC), Astronomy and Astrophysics Research and Development, Addis Ababa, Ethiopia
[2]Department of Physics, College of Natural Sciences, Jimma University, Jimma, Ethiopia

Email address:
gemechumk@gmail.com (Gemechu Muleta Kumssa)
[*]Corresponding author

To cite this article:
Gemechu Muleta Kumssa, Solomon Belay Tessema. (2023). Protoplanetary Disk Formation in a Self-gravitating Molecular Cloud. *International Journal of Astrophysics and Space Science, 11*(2), 23-37. https://doi.org/10.11648/j.ijass.20231102.12

Received: October 19, 2023; **Accepted:** November 2, 2023; **Published:** November 30, 2023

Abstract: The formation of the protoplanetary disc is a crucial step in planetary system formation. The study of protoplanetary disk formation is important for understanding the origins of our solar system as well as planets orbiting other stars. Many studies of protoplanetary disc formation focus on the initial properties of the planetary disc, such as mass, radius, and density, rather than the parent cloud properties. As a result, we're looking into the formation of the protoplanetary disc in the context of the central star-forming core and the parent cloud parameters. Thus we derive numerical results from the theoretical model using boundary conditions, confirming the presence of a correct link between the features of the developing disk, parent cloud, and central core. In theory, we model the disc's mass, density, and temperature in terms of the parent cloud and the center core's attributes. In addition, using the mass-momentum transfer method in conjunction with the newly formulated disc mass and the associated host star, we determine the masses of the disk and core. We also explain how the magnetic field affects disc formation by formulating the mass of the disc formed from a magnetized cloud. The findings reveal that the properties of the parental cloud and the host star have a significant impact on the formation of a protoplanetary disc and its essential dynamic parameters, such as mass, surface density, and mass density.

Keywords: Molecular Cloud, Self-gravitating, Protostellar Core, Protostar, Protoplanetary Disk, Planetary System, Accretion

1. Introduction

The rotating disk of dense gas surrounding a young, newly formed star is termed the protoplanetary disk. As described by [3] stars form out of relatively dense volumes of molecular gas, typically denser than $\sim 10^4 cm^{-3}$, generally named cores. The Keplerian and "moderately thin disk" have an approximate "aspect ratio" (H/R) of ~ 0.1 [27]. A protostar is created when gravity collapses the molecular cloud core, preserving angular momentum and creating a protostar surrounded by a disk.

Through the lifetime of the disk, which is a few million years, much of the disk mass drains on to the central protostar, while some forms protoplanetary disks and condenses into planets, some of which can be ejected or accreted by the central star, and some are lost to outflows (e.g. protostellar jets, photoevaporative winds, and magnetic winds). In this paper, we refer to the parent cloud core or pre-stellar core, which is the site of protostellar to protoplanetary disk formation.

Cores are narrow scale disintegrated from MC, and clumps are nearly medium-sized MC, which is the place of diversified star-making domains in addition to many protoplanetary disks [16]. As defined by [31] the disk formation takes place in a disorder-persuaded and powerfully magnetized cloud core. In this work, we need to explore disk formation in self-gravitating clouds and magnetic fields also.

Pre-stellar cores are formed when molecular clouds fragment into self-gravitating cores. These cores collapse and form a protostar surrounded by a disk of gas (a protostellar disk) near their centres. Initially, these protostars are large in size (AU-size). According to [7], typical masses of pre-stellar cores in low-mass star-forming regions such as Taurus

and Ophiuchus range from $\sim 0.5M_{\odot}$ to $\sim 10\ M_{\odot}$. However, the relationship between the pre-stellar core (parent cloud core) and the protoplanetary disk is not yet well modelled theoretically and calculated numerically. Here we mainly focus on small-scale fragments fragmented from MC, which are the sites of a single star and its protoplanetary disk formation. Planets form from protoplanetary disks of gas and dust [4] Without knowing how protoplanetary disks form, we cannot understand the formation of planets. This necessitates studying the relationship between disks and their parent MC core.

How the disk mass, density, and temperature can be expressed in terms of the envelope (parent cloud) and central core (stellar object) properties in disk assembly time is not well described. Infrared-dark cores are the birthplaces of high-mass stars, with masses of up to $\sim$ 100 $M_{\odot}$, radiuses of only 0.1 pc or less, and densities of up to $\sim 10^{12}$ hydrogen molecules m^{-3} [7]. Even though the significant role of the properties of this core in forming the protoplanetary disk has not yet been described, [35] discovered that the the maximum density ρ_{max} within the core remains below $\rho_{\star} = 10^{-11} gcm^{-3}$ during the phase studied, and he calculated the radius at which the disk mass contained approximately 50% with ($\rho_{\star} > \rho > 10^{-16} gcm^{-3}$ as well as obtained the lowest density threshold of protostars is $\rho = 10^{-16} gcm^{-3}$ and the highest density threshold is $\rho = 10^{-13} gcm^{-3}$.We adopt these values of disk density to generate a numerical value from our theoretical model. Moreover, [26] described the stellar accretion rates and disk mass relations for Ophiuchus sources. But the relationship between parent cloud properties and the protoplanetary disk was not taken into consideration.

Because protostellar disks (PSDs) have a considerable size, they do not confine themselves solely to 10 AU or 20 AU but instead expand to hundreds of thousands of AU. Therefore, we use the terms both large-scale and small-scale protostellar disks to characterize their formation. A disk of mass $M_{disk} \sim 1M_{\odot}$ was observed by [10]. However, the mass of the protostellar disk with respect to the nature of the parent cloud core has not been theoretically formulated. On the other hand, [25] pointed out that the mass of the central protostellar core is $\sim 0.01 - 0.1M_{\odot}$. Furthermore, regarding the properties of protoplanetary disk, [28] calculated the radial gas temperature profile T(r) of the HL tau disk using the surface brightness profile data of the optically thick bright ring provided by [1]. However, the relationship between the temperature of the protoplanetary disk and the mass and size of the core has not yet been elucidated. Moreover, [33] demonstrated the correlation between the mass of the disk and the rate of accretion in the case of Lupus [2, 14, 18]. However, the impact of the parent cloud or envelope's properties and the hosting star on the final mass of the protoplanetary disk has not been comprehensively explained in theory. Consequently, there exists a void in the understanding of the association between the protoplanetary disk, the parent MC core, and the hosting star. Hence, we aim to contribute to bridging this knowledge gap.

In this way, we first calculate the critical mass of the self-gravitational MCc from the energy generated during free fall and then control the core accretion velocity. We assume that the mass accretion rate of the protostar approximates the accretion rate of the disk. Then, using the parameters of the parent cloud and the star-forming core, the surface density of the disk is calculated and the mass of the disk is calculated. The disc mass is determined numerically using the parameter spacing. To relate the mass of the primary star to the mass of the surrounding disk, we use the disk mass determined numerically by the momentum equation. We then use the disk formed in the slightly magnetized environment to calculate the mass and angular momentum of the disk.

This article is structured as follows: In section 2, we outline the fundamental equations and assumptions that we will use in our modeling. In section 3, we theoretically derive equations for the surface density, mass, density, and temperature of the disk based on the properties of the parent MC core, central core, and the time of disk formation. In subsection 3.5, starting from the equation of momentum transport, we explain the connection between the central star and the protoplanetary disk, as well as the properties of the parent molecular cloud. In subsection 3.6, we compute numerical values for a non-magnetized disk by applying values to the parameters in the model equation. In subsection 3.7, we model the mass, density, and momentum of a disk formed in a magnetized cloud. In Section 4, we analyze and discuss our findings. Finally, we present our conclusion in Section 5.

2. Theoretical Background

In this portion, we explain the disk accretion and the core accretion relying on the fundamental equations for steady disk surface density.

2.1. Disk Accretion and Core Accretion

We assume a steady-state accretion disk beginning from the surface density of the spherical disk described as

$$\Sigma_{\mathrm{d}} = \frac{M_{\mathrm{d}}}{\pi R_{\mathrm{d}}^2} \tag{1}$$

Where Σ_d represents disk surface density,M_d represents disk mass, and $R_d$represents disk radius, Then

$$M_d = \pi R_d^2 \Sigma_d \tag{2}$$

$$dM_d = 2\pi R_d \Sigma_{_d} dR_d \tag{3}$$

Dividing both sides by dt we have

$$\frac{dM}{dt} = \frac{d}{dt}(2\pi R_d \Sigma_d R_d) = 2\pi R_d \Sigma_d \frac{dR_d}{dt} \tag{4}$$

yields

$$\dot{M}_d \simeq 2\pi R_d v_r \Sigma_{_d} \tag{5}$$

Where $\dot{M}_d$ is the rate of disk accretion, v_r is the inflow

(radial) velocity by agreement, and positive v_r is in the outward direction, accretion has a velocity less than zero $v_r < 0$. If v_r = 0, the disk is non-viscous.As [12] described the local viscous time scale can be written as $t_\nu(r) = r/v_r$. The infall is due to accretion of matter. Such accretion enable the outward transport of angular momentum and the inward transport of mass. In the absence of other processes, viscous processes attempt to establish a quasi-steady state in which the local accretion rate $\dot{M}_{(r)}$ is independent of radius over a large portion of the disk.

2.2. The Initial Mass of the Collapsing Cloud

The total gravitational energy released when a cloud contracts is $\Delta E = \frac{3GM_c^2}{10R_c}$, assuming a spherical molecular cloud with an average density of rho_c. Using the method developed by [11], where $0 < \epsilon < 1$ is quantified as the ratio of radiation luminosity to gravitational energy released per unit time (gravitational luminosity) as $\epsilon = \frac{L_{rad}}{L_{gf}}$, $L_{gf} = \frac{dE}{dt_{ff}}$, $L_{rad} = 4\pi R_c^2 \sigma T_c^4$, $t_{ff} = \left[\frac{3\pi}{32G\rho_c}\right]^{\frac{1}{2}}$. Adopting the technique of calculating critical mass in a paper by [11] and basic equations therein as well as performing all the necessary procedures through equating radiation luminosity and gravitational luminosity of self-gravitating MC as $\epsilon L_{gf} = L_{rad}$ then doing some mathematical manipulation we find $M_c \approx 1.7174 \times 10^4 \left(\frac{R_c^9 T_c^8}{\epsilon^2}\right)^{\frac{1}{5}} kg = 8.587 \times 10^{-27} \left(\frac{R_c^9 T_c^8}{\epsilon^2}\right)^{\frac{1}{5}} [M_\odot]$. This is the minimum mass of self-gravitating clouds needed for collapse. In this paper, we use $M_\odot \approx 2 \times 10^{30}$ kg. Furthermore, assuming a spherical system and formulating the relationship between a parent cloud of mass $M(R) = \rho_{(R)} \frac{4\pi R^3}{3}$ and an inner core of mass $M(r) = \rho_{(r)} \frac{4\pi r^3}{3}$, where taking the ratios of M (r) to M (R) and substituting M (R) instead of M_c, we re-describe the protostellar core mass in terms of the parent cloud properties as

$$M_{core} \approx 1.7174 \times 10^4 \left[\frac{T_c^8}{\epsilon^2 R_c^6}\right]^{1/5} \frac{r^3 \rho_{(r)}}{\rho_c}, \tag{6}$$

Where M_c = $M(R)$, R = R_c, ρ_r = ρ_{core}, $\rho_{(R)} = \rho_c$ are parent cloud properties with a density of ρ_c. We find the core accretion rate and approximate it to the disk accretion rate to solve for the disk mass as well as disk density in terms of disk formation time and dimensionless efficiency factor ϵ.

2.3. Protostellar Core Accretion

We assume that the accretion rate throughout the protostellar disk is constant over time and is determined by the core's growth rate. At the boundary, the mass falling onto the core is approximated to be the same as the mass gained by the disk from the envelope. Approximating the accretion rate of the protostellar disk to the rate of mass falling onto the central core is not through the entire lifetime but up to the protostar separation time from the surrounding disk. After the disk separated from the central young stellar object, it would become a protoplanetary disk. Then, after the formation of the protoplanetary disk, the accretion rate of the protoplanetary disk is different from the central star growth rate. This is in line with the statement provided as the dusty disks persist around most low-mass stars for a Myr or more, much longer than the lifetime of the natal molecular core. At the stage where the protostellar core is dispersed, the now optically visible central star has nearly achieved its final mass, and the disk is no longer protostellar, but it may still be protoplanetary [20]. As explained in the paper by [20] in the literature of young stellar objects (YSOs), this corresponds to physical stage II [30].

In this study, we will continue to use the term "protostellar core" to refer to the central star-forming region (the very early stage in the evolution of a star) in the middle of the protostellar disk that continues to grow by accretion of the surrounding material to eventually form a star. A protostellar disk is created as the gas and dust of a stellar nursery collapse gravitationally in a process that eventually creates stars and planetary systems. As the gas clumps together at the centre of the cloud, physical forces pull it into a spinning disk. The core growth rate in free-fall time of self-gravitating MC is then formulated as

$$\dot{M}_{acc} \approx \frac{dM_{core}}{dt_{ff}} \approx \frac{M_{core}}{t_{ff}} \tag{7}$$

where $t_{ff} = \sqrt{\frac{3\pi}{32G\rho_c}}$ is free-fall time.

$$\dot{M}_{acc} \approx \frac{1.2 \times 10^4 \left[\frac{T_c^8}{\epsilon^2 R_c^6}\right]^{1/5} \frac{r^3 \rho_r}{\rho_c}}{t_{ff}} \tag{8}$$

Equation (8) implies the mass infall rate depends on different factors arising from the properties of the envelop and the central core, multiplying Eqn. (8) by $\frac{\sqrt{\rho_c}}{\sqrt{\rho_c}}$ we get

$$\dot{M}_{acc} \approx 3.2 \times 10^4 \left[\frac{T_c^8}{\epsilon^2 R_c^6}\right]^{1/5} \left(\frac{G}{\rho_c}\right)^{1/2} r^3 \rho_r \tag{9}$$

$$\dot{M}_{acc} \approx 3.2 \times 10^4 \left(\frac{G}{n_c \mu m_H}\right)^{1/2} \left[\frac{T_c^8}{\epsilon^2 R_c^6}\right]^{1/5} r^3 \rho_r \tag{10}$$

Where R_c, n_c, and T_c the radius, particle number per unit volume, and temperature of the pre-stellar core, respectively. Eqn. (10) is the growth rate of the star-forming core at the centre of a protostellar disk. The gas pressure is $P = \frac{\rho K_B T}{\mu m_H} = n_c K_B T_c$, and the mean molecular weight of the particle is ($m_H = 1.67 \times 10^{-27}$ kg = atomic mass unit), and $\mu = 2.36$ in the atomic mass unit. For simplicity, we assume the thermal pressure is the same as the gas pressure at the boundary of the disk and the parent cloud. This implies $P_{g,r} \sim \rho_r c_{sr}^2$ at the intersection of two regions (parent cloud and protostellar disk). Then we have

$$\dot{M}_{acc} \approx 3.1646 \times 10^4 \left[\frac{GK_B}{\rho_c c_{sR}^2 \mu m_H}\right]^{1/2} \left[\frac{T_c^{7/2}}{\epsilon^2 R_c^6}\right]^{1/5} \times r^3 \frac{\rho_r c_{sr}^2 \mu m_H}{K_B T_r} \tag{11}$$

where c_{sR} and c_{sr} are parent MC (the envelope) and core sound speeds, respectively. whereas $\dot{M}_{acc}$ is the rate of accretion given in kg yr^{-1} or $M_\odot yr^{-1}$ depending on the units used in this study to calculate parameters and substitute constants. Then we have

$$\dot{M}_{acc} \approx 3.1646 \times 10^4 \left[\frac{G\mu m_H}{\rho_c c_{sR}^2 K_B}\right]^{1/2} \left[\frac{T_c^{7/2}}{\epsilon^2 R_c^6}\right]^{1/5} r^3 \frac{\rho_r c_{sr}^2}{T_r} \tag{12}$$

The conditions in the parent cloud (envelope or protostellar disk) and the properties of the central protostellar core with temperature T_r control the property of $\dot{M}_{acc}$. This indicates how important the parent cloud core properties are in understanding disk properties.

3. Results

In this section, we formulate our own model from the basic equations and conditions we have set earlier.

3.1. Surface Density of a Disk in a Non-magnetized Cloud

We consider steady state disks and conservation of momentum. Consequently, assuming that the accretion rate of the inner disk is approximately the same as the central protostellar core growth rate, Then, using Eqns. (12) and (5) we have

$$\Sigma_{gaes+dust} = \frac{3.1646 \times 10^4 \left[\frac{G\mu m_H}{\rho_c c_{sR}^2 K_B}\right]^{1/2} \left[\frac{T_c^{7/2}}{\epsilon^2 R_c^6}\right]^{1/5} r^3 \frac{\rho_r c_{sr}^2}{T_r}}{2\pi R_d v_r} \tag{13}$$

Where v_r is the radial velocity of infalling matter across the disk and $\Sigma_{gas+dust}$ = Σ_d is the density of the disk surface in $[kgm^{-2}]$. after simplifying Eqn. (13) we arrive at

$$\Sigma_{gaes+dust} = 5.0366 \times 10^3 \frac{\left[\frac{G\mu m_H}{\rho_c c_{sR}^2 K_B}\right]^{1/2} \left[\frac{T_c^{7/2}}{\epsilon^2 R_c^6}\right]^{1/5} r^3 \frac{\rho_r c_{sr}^2}{T_r}}{R_d v_r} \tag{14}$$

In terms of disk formation time, the surface density is expressed as

$$\Sigma_{gaes+dust} = 5.0366 \times 10^3 \frac{\left[\frac{G\mu m_H}{\rho_c c_{sR}^2 K_B}\right]^{1/2} \left[\frac{T_c^{7/2}}{\epsilon^2 R_c^6}\right]^{1/5} r^3 \frac{\rho_r c_{sr}^2}{T_r}}{t_{cr} v_r^2} \tag{15}$$

Here we show in Eqn (15) Σ is parametrized as a radial power law $\Sigma \propto R_d^{-p}$, which agrees with observational p values measured in the 0.5 to 1.5 range [34]. We use a simple method to distinguish the surface density of the protostellar disk from the protoplanetary disk: if R_d = r, the core and disk are not detached from each other, we call it a protostellar disk. If $R_d \neq$ r (i.e $R_d >$ r), the core is separated from the disk and is now in protoplanetary disk form.

3.2. Disk Mass in a Non-magnetized Cloud

A disk forms very early on and grows rapidly during the Class 0 collapse phase. A protostellar disk will form into a protoplanetary disk in time. Thus, the disk mass depends on time until accretion stops. Hereafter, we explain the mass of the disk using disk assembly or formation time, beginning from the first gravitational collapse phase of the initial MC core (pre-stellar core) ($t_{ass} \approx 0$) to planetary system formation time ($t_{ass} \geqslant 10^7$ yrs). For simplicity, we consider that a disk's surface density is constant over radius at a given instant in time for the given thin disk.

We consider disk formation time sim and assembly time (t_{ass}), estimating $t_{ass} = \frac{R_d}{v_r}$. We take into account that $t_a ss$ in the outer disk is of order the disk age, $t_a ss$ (i.e. the disk has only recently grown to its current size). The outer disk's timescale t_{ass} is similar to the local viscous timescale $t_\nu(r)$ [5, 6, 8, 34]. This shows that disks have been shaped by viscous evolution. It is worth noting that as $t_a ss$ increases, either the disk radius or the speed of infalling matter through the disk increases. At the final time of disk formation, the speed of infalling matter becomes very slow and finally stops. Therefore, the formation time mostly depends on the speed of infalling matter through the disk and the disk radius. whereas the radial speed of infalling matter is influenced by disk density. For these reasons, longer assembly time doesn't necessarily mean a larger disk. By replacing $P_r \sim \rho_r c_{rs}^2$ and assuming the gas pressure is $\approx$ thermal pressure at the surface of the protostellar core.

The larger t_ass indicates that the speed of matter flowing out of the disk and onto the central stellar object is very slow. On the other hand, as the time taken to assemble the disk by gaining matter from the envelope is relatively larger, the possibility of getting a more massive disk increases. Hereafter, t_{ass} is the disk assembly time assumed to be similar to the disk formation time (t_{fr}). The radius, density, and temperature of the central protostellar core are given by r, ρ_r, and T_r, respectively. Since we considered the core growth rate and disk accretion rate to be almost similar at the boundary, Therefore, from Eqns. (12, 2 and 13), we get

$$M_d \approx 3.1646 \times 10^4 \left[\frac{G\mu m_H}{\rho_c c_{sR}^2 K_B}\right]^{1/2} \left[\frac{T_c^{7/2}}{\epsilon^2 R_c^6}\right]^{1/5} \times r^3 \frac{\rho_{(r)} c_{sr}^2}{T_r} \frac{1}{2\pi R_d v_r} \pi R_d^2 \tag{16}$$

The thermal pressure in the parent cloud core (pre-stellar core) is $\rho_c c_{sR}^2$, which is similar to the gas pressure at the pre-stellar core's surface. The pre-stellar core properties are used as the envelope properties. From Eqn.(16) we get

$$M_d(t_{ass}) \approx 1.5823 \times 10^4 \left[\frac{G\mu m_H}{K_B \rho_c c_{sR}^2}\right]^{1/2} \left[\frac{T_c^{7/2}}{\epsilon^2 R_c^6}\right]^{1/5} \times \frac{\rho_{(r)} c_{sr}^2}{T_r} r^3 t_{ass} \tag{17}$$

This is the mass of embedded protostellar disks with substantial circumstellar envelopes. The envelope properties are the properties of the parent MC $\left(\left[\frac{T_c^{7/2}}{\epsilon^2 R_c^6}\right]^{1/5} \ \& \ \rho_c c_{sR}^2\right)$. The mass of the protostellar disk is inversely proportional to the pressure of turbulence in the parent MC core (pre-stellar core) and directly proportional to the pressure of turbulence in the protostellar core($M_d \propto P_R^{-1/2}$ and $M_d \propto P_r = \rho_r c_{sr}^2$). This confirms the idea that turbulence halts collapse at a large scale but fevers collapse at a small scale. Thus, our model is in agreement with the current understanding of turbulence's role in star formation as well as protostellar disk formation. As a result of this, $M_d \propto T_c^{7/10}$, $M_d \propto T_r^{-1}$, $M_d \propto R^{-6/5}$, $M_d \propto t_{ass}$ & $M_d \propto r^3$ of these parameters and the dynamical process governs the formation of a protostellar disk.

The transition period from protostellar disk to protoplanetary disk depends on the disk's assembly time. Eqn.(17) shows the relation between the disk's mass and the properties of the pre-stellar core (parent cloud core). In other words, the protostellar core (protostar) radius r is $\sim R_d$ at a very early time ($t_{ass} \ll 1$ million) years of disk formation). Which means, at the very early formation time, the protostar is not completely detached from its envelope. As a result, we can rewrite M_d as

$$M_d(t_{ass}) \approx 1.5823 \times 10^4 \left[\frac{G\mu m_H}{K_B \rho_c c_{sR}^2}\right]^{1/2} \left[\frac{T_c^{7/2}}{\epsilon^2 R_c^6}\right]^{1/5} \times \frac{\rho_{(r)} c_{sr}^2}{T_r} \frac{R_d^4}{v_r} \tag{18}$$

In the collapse of MC, the first core (pre-stellar core) forms before the protostar. At this time, the first core displays a thick disk like arrangement. After the protostar formation, the core slowly transforms into a thin disk similar to the protostellar disk. Therefore, at its formation stage, the protostellar disk size is almost the same as the first core size. Here, the first core is the initial molecular cloud core fragmented from the giant cloud. Finally, the disk mass depends on time and can be described as

$$M_d(t_{ass}) \approx 1.1 \times 10^{-3} \left[\frac{1}{\rho_c c_{sR}^2}\right]^{1/2} \left[\frac{T_c^{7/2}}{\epsilon^2 R_c^6}\right]^{1/5} \times \frac{\rho_{(r)} c_{sr}^2}{T_r} R_d^3 \, t_{ass} \tag{19}$$

For example, if the parameters, if parameters $\rho_c = 10^{-14} kgm^{-3}$, $c_{sR} = 332 ms^{-1}$, T_c = 10K, R_c = 0.01pc, ϵ = 0.5, c_{sr} = 300ms^{-1}, T_r = 100K, R_d = 100AU, $t_{ass} \approx 5 \times 10^3$ yr, $\rho_r = \rho_{core} \sim 10^{-9} kgm^{-3}$ the disk mass is $\sim 4.4198 \times 10^{28}$ kg = $0.0923 M_\odot$. Thermodynamic properties of the disk forming cloud core influence the final disk mass. The disk mass we estimated here is in agreement with results obtained by many authors.

For example, [23] found that the proplyd disk masses in Orion range up to 0.078 $M_\odot$. Many disks have masses in the order of 0.001 $M_\odot$. In addition, [23] detected five sources that are more massive than 0.01 $M_\odot$. Moreover, [24] surveyed NGC 2024 (age $\sim$ 0.5 Myr) and found a greater fraction of disks with masses exceeding 0.01 $M_\odot$ as well as estimated disk masses 0.03-0.05 $M_\odot$. Therefore, our model will help calculate the disk's mass from the parent cloud and the central core parameters. According to our model (Eqn.(19)) the mass of the disk depends on time until accretion ceases. Thus, the disk mass depends on time until accretion stops. We explain the mass of the disk using disk assembly or formation time,

beginning from the first gravitational collapse phase cloud core ($t_{ass} \approx 0$) to planetary system formation time ($t_{ass} \geqslant 10^7$ yrs). The radial velocity of infalling matter from Eqn.(17) at the time r $\neq R_d$ is

$$v_r \approx 1.5823 \times 10^4 \left(\frac{G\mu m_H}{\rho_c c_{sR}^2 K_B}\right)^{1/2} \left(\frac{T_c^{7/2}}{\epsilon^2 R_c^6}\right)^{1/5} r^3 \frac{\rho_{(r)} c_{sr}^2}{T_r} \frac{R_d}{M_d} \tag{20}$$

Assuming a spherical disk with density ρ_d=$n_d \mu m_H$ & radius to mass ratio $\sim$ 3/4$\pi R_d^2 \rho_d$. Then Eqn.(20) becomes

$$v_r \approx 3.7775 \times 10^3 \left(\frac{G\mu m_H}{\rho_c c_{sR}^2 K_B}\right)^{1/2} \left(\frac{T_c^{7/2}}{\epsilon^2 R_c^6}\right)^{1/5} \times \frac{\rho_{(r)} c_{sr}^2}{T_r} \frac{r^3}{R_d^2 \rho_d} \tag{21}$$

The radial flow of matter in the disk depends both on the envelope and central core properties. According to [7], the median disk mass for embedded protostellar disks with substantial circumstellar envelopes (class I) and pre-main-sequence stars with a surrounding disk but little or no remaining envelope (class II) is approximately 1% of the stellar mass (i.e., $\sim$ 5-10M_{Jup}). We adopt this conceptual framework to formulate the disk's mass, density, temperature, etc.

From Eqn.(21) the disk density of a non-magnetized cloud in terms of parent cloud property and central core property is expressed as

$$\rho_d \approx 3.7775 \times 10^3 \left(\frac{G\mu m_H}{\rho_c c_{sR}^2 K_B}\right)^{1/2} \left(\frac{T_c^{7/2}}{\epsilon^2 R_c^6}\right)^{1/5} \times \frac{\rho_{(r)} c_{sr}^2}{T_r} \frac{r^3}{R_d^2 v_r} \tag{22}$$

In terms of disk assembly, we get

$$\rho_d \approx 2.6082 \times 10^{-4} \left(\frac{1}{\rho_c c_{sR}^2}\right)^{1/2} \left(\frac{T_c^{7/2}}{\epsilon^2 R_c^6}\right)^{1/5} \times \frac{\rho_{(r)} c_{sr}^2}{T_r} \frac{r^3}{R_d^3} t_{ass} \tag{23}$$

The density depends not only on the disk time assembly, which is estimated from the disk formation time, but also on the properties of the central core and its envelope. The pressure in the central core helps the disk's density to rise, whereas pressure in the envelope reduces the disk's density. This indirectly confirms that thermal pressure on a small scale supports gravity but counteracts gravity on a large scale. Since the supersonic thermal kinetic energy stabilizes the clouds on large scales and prevents global collapse, and its shock induces local compressions, [9, 21, 22]. At the very early time of disk formation, the central core radius r and the disk radius R_d may not be different (there is no clear boundary between the central core size and the disk size). As a result, using Eqn. (ref eqn:23), one can calculate the disk density using this approximation (r = R_d).

3.3. Disk Temperature

The gravitating body grows in mass by accumulating matter from an external reservoir. Accretion is illustrated by considering a test mass m in the gravitational field of a spherically symmetric body with mass M and radius R ($m << M$) [19]. The accretion of gas generates gravitational energy, part of which goes into further heating of the core and part of which is radiated away, providing the luminosity of the accretor core given by the standard equation [19].

$$L_{acc} = \frac{GM_{core}\dot{M}_{core}}{2R_{core}} \tag{24}$$

where M_{core} and R_{core} are the mass and radius of the central protostellar core, respectively, and M_{core} and R_{core} is the central core's mass accretion rate. The factor of 1/2 originates from the fact that half of the potential energy is dissipated in the accretion disk. Initially, H_2 in the core loses energy by being in thermal balance with the dust. Impacts with dust grains transfer thermal energy from the gas to the dust, which is then able to radiate that energy away as a black body [17, 29]. If the dominant source of luminosity is accretion after the disk has started accreting matter from its circumstellar envelope, radiation luminosity is balanced with accretion luminosity to formulate the temperature of the disk. Now approximating the accretion luminosity is the same as the radiation luminosity of the disk. Thus

$$L_{acc} = \frac{GM_{core}\dot{M}_{core}}{2R_{core}} = 4\pi\sigma R_d^2 T_d^4 \tag{25}$$

Using Eqn.(12) in Eqn.(25), we have

$$T_d^4 = \frac{3.1646 \times 10^4 GM_r \left[\frac{G\mu m_H}{\rho_c c_{sR}^2 K_B}\right]^{1/2} \left[\frac{T_c^{7/2}}{\epsilon^2 R_c^6}\right]^{1/5} r^3 \frac{\rho_{(r)} c_{sr}^2}{T_r}}{8\pi\sigma R_{core} R_d^2} \tag{26}$$

Where M_r is the central core mass, r=R_{core} is the core radius, T_r is the core temperature.

$$T_d \approx \left[\frac{3.1646\times10^4 GM_r\left(\frac{G\mu m_H}{\rho_c c_{sR}^2 K_B}\right)^{1/2}\left(\frac{T_c^{7/2}}{\epsilon^2 R_c^6}\right)^{1/5}}{8\pi\sigma R_d^3}\right]^{1/4}\times\left(\frac{r^3\rho_r c_{sr}^2}{T_r}\right)^{1/4} \tag{27}$$

To obtain the temperature of the disk, we divide the disk formation time into phases. For the first phase, we consider the early formation time of the disk and assume that $R_d \approx R_{core}$ = r. Then in the first collapse phase, from the relationship we have

$$T_{psd} \approx \left[\frac{3.1646\times10^4 M_r\left(\frac{G^3\mu m_H}{\rho_c c_{sR}^2 K_B}\right)^{1/2}\left(\frac{T_c^{7/2}}{\epsilon^2 R_c^6}\right)^{1/5}}{8\pi\sigma}\right]^{1/4}\times\left(\frac{\rho_r c_{sr}^2}{T_r}\right)^{1/4} \tag{28}$$

Eqn.(28) shows the disk temperature is independent of the disk radius in this stage. Using Eqn. (ref eqn: 27), the disk temperature in terms of the disk assembly time for $R_d \sim$ r is

$$T_{psd}(t_{as}) \approx \left[\frac{3.1646\times10^4\left(\frac{M_r^2 G^3\mu m_H}{\rho_c c_{sR}^2 K_B}\right)^{1/2}\left(\frac{T_c^{7/2}}{\epsilon^2 R_c^6}\right)^{1/5}}{8\pi\sigma v_r t_{ass}}\right]^{1/4}\times\left(r\frac{\rho_{(r)} c_{sr}^2}{T_r}\right)^{1/4} \tag{29}$$

We assume $R_d \neq R_{core} = r$ after the protoplanetary disk separates from the central protostar (because the disk flattens to conserve momentum while the core remains at the disk's center) for the second phase. The temperature of the protoplanetary disk (T_{ppd}) is now calculated using Eqn. (ref eqn. 26).

$$T_{ppd} \approx \left[\frac{3.1646\times10^4\left(\frac{M_r^2 G^3\mu m_H}{\rho_c c_{sR}^2 K_B}\right)^{1/2}\left(\frac{T_c^{7/2}}{\epsilon^2 R_c^6}\right)^{1/5} r^3\frac{\rho_{(r)} c_{sr}^2}{T_r}}{8\pi\sigma R_d^2 v_r t_{ass}}\right]^{1/4} \tag{30}$$

When the circumstellar disk is separated from the central protostar (as in the case in Eqn. (30)) $T_d \propto R_d^{-1/2} v_r t_{ass}^{-1/4}$. This implies that the temperature of the protostellar & the protoplanetary disk will be described in different ways, so that there may not be a general and specific solution to the disk's temperature. Hence $\sigma = 5.67\times10^{-8} Js^{-1}\ m^{-2}K^{-4}$, K_B =1.38 $\times10^{-23}$ j/k, $m_H = m_p$ = 1.67 $\times10^{-24}$ g, μ = 2.36 m_H, G= 6.67 $\times10^{-11} m^3 kg^{-1} s^{-2}$. After simplifying Eqn.(30), the protoplanetary disk temperature interms of disk formation time is described as

$$T_{ppd}(t_{ass}) \approx 1.26\times10^{-2}\left[\frac{\left(\frac{M_r^2}{\rho_c c_{sR}^2}\right)^{1/2}\left(\frac{T_c^{7/2}}{\epsilon^2 R_c^6}\right)^{1/5} r^3\frac{\rho_{(r)} c_{sr}^2}{T_r}}{R_d^2 v_r t_{ass}}\right]^{1/4} \tag{31}$$

Eqns.(30) and (31) show that as the disk's age increases, its temperature drops. This confirms that disks' temperatures are very high in the early stages due to material infall, which is aligned with numerical models of non-magnetic collapsing molecular cores [15]. This implies that, as the envelope material is used up or dispersed, the disk cools down. This shows the validity of our model. As soon as accretion begins at the protostellar phase, the rapid inside-out gravitational collapse of molecular cloud cores conserves angular momentum, producing a protostar surrounded by a disk and an optically thick infalling envelope. It is at this stage that the mass growth of the central core increases more than the mass growth of the disk surrounding it. Thus, the mass of the protostar and the circumstellar disk will be different after a long time accretion process. Due to this fact, the disk's temperature varies and depends on the disk's formation time.

3.4. Dust Surface Density

To approximate the mass of planets, especially terrestrial planets formed from the total disk, we assume a gas to dust ratio of 100:1, such that Σ_{dust} = 0.01 $\Sigma_{gas+dust}$ throughout the disk. In our case, surface density of the gas in the disk (Σ_{gas}) is $\sim$ disk's surface density (Σ_{disk}). Now having this concept in mind and using Eqn.(13), the dust surface density is described as

$$\Sigma_{dust} = 0.01 \frac{3.1646 \times 10^4 \left[\frac{G\mu m_H}{\rho_c c_{sR}^2 K_B}\right]^{1/2} \left[\frac{T_c^{7/2}}{\epsilon^2 R_c^6}\right]^{1/5} r^3 \frac{\rho_r c_{sr}^2}{T_r}}{2\pi R_d v_r} \tag{32}$$

Finally, we have the surface density, which would be involved in rocky planet formation in the disk described as

$$\Sigma_{dust} \approx 3.4775 \times 10^{-6} \frac{\left[\frac{1}{\rho_c c_{sR}^2}\right]^{1/2} \left[\frac{T_c^{7/2}}{\epsilon^2 R_c^6}\right]^{1/5} r^3 \frac{\rho_r c_{sr}^2 t_{ass}}{T_r}}{R_d^2} \tag{33}$$

This indicates the probability of forming rocky planets is influenced by the composition and properties of the pre-stellar core in addition to external agents that we did not incorporate in this paper for the time being.

3.5. Angular Momentum Transfer

The accretion of material onto the newly forming star must be accompanied by an expansion of the remaining disk material to conserve angular momentum. Infalling of matter continues until the disk hosting star gets enough temperature, density and mass to fuse hydrogen. In the process of mass infall momentum flow out, consequently momentum is conserved. This leads to formation of protoplanetary disk which will be site for planets formation. In the process of accretion, angular momentum must be lost from, or redistributed within the disk gas and this process turns out to require time scales that are much longer than the orbital or dynamical time scale [4].

We apply the simplest angular momentum transfer method to formulate an equation for the mass of a star in terms of parent cloud, disk formation time, protostellar core parameters, and disk radius. Thus, the standard equation of angular momentum is written as $dJ_d = \Omega_d dI_d$. using the angular momentum transport equation for the spherical disk of radius R_d rotating with angular velocity Ω_d. This is integrated as $J_d = \int \Omega_d R_d^2 \, dm$, Where I_d is the disk's moment of inertia, R_d is its radius, J_d is its angular momentum, and M_d is its mass [13] $\Omega_d = \sqrt{\frac{GM_\star}{R_d^3}}$ denotes the angular velocity of the disk, dm_d is an element of mass in the disk, and $M_\star$ is the stellar mass. We get $J_d = \left(\frac{GM_\star}{R_d^3}\right)^{1/2} R_d^2 \int_0^{M_d} dm_d$. Assuming that as soon as gravitational collapse begins the disk age t=0 $\Rightarrow m_d \to 0$ and after some time t, the disk formation begins then $m_d \to M_d$, thus

$$J_d = (GM_\star R_d)^{1/2} M_d \approx 1.1 \times 10^{-3} (GM_\star R_d)^{1/2} \left[\frac{1}{\rho_c c_{sR}^2}\right]^{1/2} \left[\frac{T_c^{7/2}}{\epsilon^2 R_c^6}\right]^{1/5} \times \frac{\rho_{(r)} c_{sr}^2}{T_r} R_d^3 \, t_{ass} \tag{34}$$

From the expression of momentum conservation $J_d = J_\star$, which can be written as $\Omega_\star M_\star R_\star^2 = \Omega_d M_d R_d^2 = (GM_\star R_d)^{1/2} M_d$. From this expression we have

$$M_d = \sqrt{\frac{M_\star}{GR_d}} \, \Omega_\star R_\star^2 \tag{35}$$

Solving for $M_\star$ and using eqn.(19) in eqn.(35) we have

$$M_\star = G \frac{R_d \left[1.1 \times 10^{-3} \left[\frac{1}{\rho_c c_{sR}^2}\right]^{1/2} \left[\frac{T_c^{7/2}}{\epsilon^2 R_c^6}\right]^{1/5} \times \frac{\rho_{(r)} c_{sr}^2}{T_r} R_d^3 \, t_{ass}\right]^2}{\Omega_\star^2 R_\star^4} \tag{36}$$

At the final stage of the protoplanetary disk and star formation as well as at the time where accretion ceases and dominated by irradiation, $\rho_{(r)} \to \rho_{(\star)}$, $c_{(r)} \to c_{(\star)}$, $T_r \to T_\star$. From this, one can calculate and show the relationship between the host star's mass and the mass of the protoplanetary disk surrounding its host star. Because we calculated the disk mass using parent cloud core and central core properties, Therefore, if we know the values of those parameters described in the disk mass equation, it is possible to guess the mass of a central star.

3.6. Numerical Rsults for Non-magnetized Disk

In this section, numerical results of disk mass have been generated using theoretical model Eqn. (19). The parameter space covered initial cloud core radius R_c = 0.01 - 1pc, temperature T_c = 10 -100K, for decreasing ϵ = 0.5-0.005 for reducing & ϵ = 0.005-0.5 for increasing one, density ρ_c = $10^{-15} - 10^{-13} kgm^{-3}$, central core temperature T_{core} = 10 - 1000K, density ρ_{core} = $10^{-9} - 10^{-7} kgm^{-3}$, disk radius R_d = 10 - 110AU, sound speed in the envelope c_{sR}= 300 - 400 ms^{-1}, sound speed in central core c_{sr} = 200 - 300 ms^{-1}, central core radius r_{core} = $1R_\odot - 100R_\odot$ and disk formation time $t_{ass} = 10^3 - 10^5$ yrs.

In Figure 1, we show that when the ratio of L_{rad} to L_g (ϵ) is reduced, the disk mass increases over time because there may not be enough radiation to disperse matter in the disk. Therefore, the disk has a high probability of attaining less mass whenever ϵ is relatively larger (more approaching to one).

Table 1. *Numerically generated results were obtained by varying physical parameters within the known ranges described in the literature using a combination of Eqns. (19) and (35).*

t_{ass} (yr)	$\rho_{(R)}$ (kgm^{-3})	R_c (pc)	M_d $(M_\odot)$	R_d (AU)	$M_\star(core)$ $(M_\odot)$	$\rho_{(r)}$ (kgm^{-3})	$r_\star$ $(R_\odot)$	$\Omega_\star$ (s^{-1})
1.000e+05	1.000e-13	1.000e-02	6.634e-08	1.000e+00	5.856e-11	1.000e-09	1.990e+00	3.162e-06
1.100e+05	9.900e-14	2.000e-02	3.282e-07	1.800e+00	6.584e-10	2.000e-09	1.980e+00	6.324e-06
1.200e+05	9.800e-14	3.000e-02	8.916e-07	2.600e+00	3.182e-09	3.000e-09	1.970e+00	9.486e-06
1.300e+05	9.700e-14	4.000e-02	1.844e-06	3.400e+00	1.022e-08	4.000e-09	1.960e+00	1.264e-05
1.400e+05	9.600e-14	5.000e-02	3.263e-06	4.200e+00	2.582e-08	5.000e-09	1.950e+00	1.581e-05
1.500e+05	9.500e-14	6.000e-02	5.221e-06	5.000e+00	5.578e-08	6.000e-09	1.940e+00	1.897e-05
1.600e+05	9.400e-14	7.000e-02	7.784e-06	5.800e+00	1.078e-07	7.000e-09	1.930e+00	2.213e-05
1.700e+05	9.300e-14	8.000e-02	1.101e-05	6.600e+00	1.921e-07	8.000e-09	1.920e+00	2.529e-05
1.800e+05	9.200e-14	9.000e-02	1.497e-05	7.400e+00	3.212e-07	9.000e-09	1.910e+00	2.846e-05
1.900e+05	9.100e-14	1.000e-01	1.972e-05	8.200e+00	5.108e-07	1.000e-08	1.900e+00	3.162e-05
2.000e+05	9.000e-14	1.100e-01	2.532e-05	9.000e+00	7.799e-07	1.100e-08	1.890e+00	3.478e-05
2.100e+05	8.900e-14	1.200e-01	3.182e-05	9.800e+00	1.151e-06	1.200e-08	1.880e+00	3.794e-05
2.200e+05	8.800e-14	1.300e-01	3.928e-05	1.060e+01	1.652e-06	1.300e-08	1.870e+00	4.110e-05
2.300e+05	8.700e-14	1.400e-01	4.777e-05	1.140e+01	2.314e-06	1.400e-08	1.860e+00	4.427e-05
2.400e+05	8.600e-14	1.500e-01	5.733e-05	1.220e+01	3.175e-06	1.500e-08	1.850e+00	4.743e-05
2.500e+05	8.500e-14	1.600e-01	6.803e-05	1.300e+01	4.279e-06	1.600e-08	1.840e+00	5.059e-05
2.600e+05	8.400e-14	1.700e-01	7.992e-05	1.380e+01	5.675e-06	1.700e-08	1.830e+00	5.375e-05
2.700e+05	8.300e-14	1.800e-01	9.307e-05	1.460e+01	7.423e-06	1.800e-08	1.820e+00	5.692e-05
2.800e+05	8.200e-14	1.900e-01	1.075e-04	1.540e+01	9.589e-06	1.900e-08	1.810e+00	6.008e-05
2.900e+05	8.100e-14	2.000e-01	1.233e-04	1.620e+01	1.224e-05	2.000e-08	1.800e+00	6.324e-05
3.000e+05	8.000e-14	2.100e-01	1.406e-04	1.700e+01	1.549e-05	2.100e-08	1.790e+00	6.640e-05
3.100e+05	7.900e-14	2.200e-01	1.593e-04	1.780e+01	1.941e-05	2.200e-08	1.780e+00	6.957e-05
3.200e+05	7.800e-14	2.300e-01	1.796e-04	1.860e+01	2.413e-05	2.300e-08	1.770e+00	7.273e-05
3.300e+05	7.700e-14	2.400e-01	2.016e-04	1.940e+01	2.977e-05	2.400e-08	1.760e+00	7.589e-05
3.400e+05	7.600e-14	2.500e-01	2.252e-04	2.020e+01	3.648e-05	2.500e-08	1.750e+00	7.905e-05
3.500e+05	7.500e-14	2.600e-01	2.506e-04	2.100e+01	4.443e-05	2.600e-08	1.740e+00	8.221e-05
3.600e+05	7.400e-14	2.700e-01	2.778e-04	2.180e+01	5.379e-05	2.700e-08	1.730e+00	8.538e-05
3.700e+05	7.300e-14	2.800e-01	3.070e-04	2.260e+01	6.477e-05	2.800e-08	1.720e+00	8.854e-05
3.800e+05	7.200e-14	2.900e-01	3.381e-04	2.340e+01	7.762e-05	2.900e-08	1.710e+00	9.170e-05
3.900e+05	7.100e-14	3.000e-01	3.712e-04	2.420e+01	9.259e-05	3.000e-08	1.700e+00	9.486e-05
4.000e+05	7.000e-14	3.100e-01	4.065e-04	2.500e+01	1.099e-04	3.100e-08	1.690e+00	9.803e-05
4.100e+05	6.900e-14	3.200e-01	4.440e-04	2.580e+01	1.301e-04	3.200e-08	1.680e+00	1.011e-04
4.200e+05	6.800e-14	3.300e-01	4.838e-04	2.660e+01	1.534e-04	3.300e-08	1.670e+00	1.043e-04
4.300e+05	6.700e-14	3.400e-01	5.260e-04	2.740e+01	1.802e-04	3.400e-08	1.660e+00	1.075e-04
4.400e+05	6.600e-14	3.500e-01	5.706e-04	2.820e+01	2.110e-04	3.500e-08	1.650e+00	1.106e-04
4.500e+05	6.500e-14	3.600e-01	6.178e-04	2.900e+01	2.464e-04	3.600e-08	1.640e+00	1.138e-04
4.600e+05	6.400e-14	3.700e-01	6.677e-04	2.980e+01	2.869e-04	3.700e-08	1.630e+00	1.170e-04
4.700e+05	6.300e-14	3.800e-01	7.204e-04	3.060e+01	3.331e-04	3.800e-08	1.620e+00	1.201e-04
4.800e+05	6.200e-14	3.900e-01	7.759e-04	3.140e+01	3.859e-04	3.900e-08	1.610e+00	1.233e-04
4.900e+05	6.100e-14	4.000e-01	8.343e-04	3.220e+01	4.461e-04	4.000e-08	1.600e+00	1.264e-04
5.000e+05	6.000e-14	4.100e-01	8.959e-04	3.300e+01	5.144e-04	4.100e-08	1.590e+00	1.296e-04
5.100e+05	5.900e-14	4.200e-01	9.607e-04	3.380e+01	5.921e-04	4.200e-08	1.580e+00	1.328e-04
5.200e+05	5.800e-14	4.300e-01	1.028e-03	3.460e+01	6.802e-04	4.300e-08	1.570e+00	1.359e-04
5.300e+05	5.700e-14	4.400e-01	1.100e-03	3.540e+01	7.801e-04	4.400e-08	1.560e+00	1.391e-04
5.400e+05	5.600e-14	4.500e-01	1.175e-03	3.620e+01	8.931e-04	4.500e-08	1.550e+00	1.423e-04
5.500e+05	5.500e-14	4.600e-01	1.254e-03	3.700e+01	1.020e-03	4.600e-08	1.540e+00	1.454e-04
5.600e+05	5.400e-14	4.700e-01	1.337e-03	3.780e+01	1.165e-03	4.700e-08	1.530e+00	1.486e-04
5.700e+05	5.300e-14	4.800e-01	1.424e-03	3.860e+01	1.328e-03	4.800e-08	1.520e+00	1.517e-04
5.800e+05	5.200e-14	4.900e-01	1.515e-03	3.940e+01	1.512e-03	4.900e-08	1.510e+00	1.549e-04
5.900e+05	5.100e-14	5.000e-01	1.610e-03	4.020e+01	1.719e-03	5.000e-08	1.500e+00	1.581e-04
6.000e+05	5.000e-14	5.100e-01	1.710e-03	4.100e+01	1.953e-03	5.100e-08	1.490e+00	1.612e-04
6.100e+05	4.900e-14	5.200e-01	1.815e-03	4.180e+01	2.216e-03	5.200e-08	1.480e+00	1.644e-04
6.200e+05	4.800e-14	5.300e-01	1.925e-03	4.260e+01	2.512e-03	5.300e-08	1.470e+00	1.676e-04

Table 1. *Continued.*

t_{ass} (yr)	$\rho_{(R)}$ (kgm^{-3})	R_c (pc)	M_d ($M_\odot$)	R_d (AU)	$M_\star$ ($M_\odot$)	$\rho_{(r)}$ (kgm^{-3})	$r_\star$ ($R_\odot$)	$\Omega_\star$ (s^{-1})
6.300e+05	4.700e-14	5.400e-01	2.040e-03	4.340e+01	2.846e-03	5.400e-08	1.460e+00	1.707e-04
6.400e+05	4.600e-14	5.500e-01	2.161e-03	4.420e+01	3.221e-03	5.500e-08	1.450e+00	1.739e-04
6.500e+05	4.500e-14	5.600e-01	2.287e-03	4.500e+01	3.643e-03	5.600e-08	1.440e+00	1.770e-04
6.600e+05	4.400e-14	5.700e-01	2.419e-03	4.580e+01	4.117e-03	5.700e-08	1.430e+00	1.802e-04
6.700e+05	4.300e-14	5.800e-01	2.557e-03	4.660e+01	4.651e-03	5.800e-08	1.420e+00	1.834e-04
6.800e+05	4.200e-14	5.900e-01	2.702e-03	4.740e+01	5.252e-03	5.900e-08	1.410e+00	1.865e-04
6.900e+05	4.100e-14	6.000e-01	2.854e-03	4.820e+01	5.927e-03	6.000e-08	1.400e+00	1.897e-04
7.000e+05	4.000e-14	6.100e-01	3.014e-03	4.900e+01	6.687e-03	6.100e-08	1.390e+00	1.928e-04
7.100e+05	3.900e-14	6.200e-01	3.181e-03	4.980e+01	7.542e-03	6.200e-08	1.380e+00	1.960e-04
7.200e+05	3.800e-14	6.300e-01	3.356e-03	5.060e+01	8.505e-03	6.300e-08	1.370e+00	1.992e-04
7.300e+05	3.700e-14	6.400e-01	3.539e-03	5.140e+01	9.589e-03	6.400e-08	1.360e+00	2.023e-04
7.400e+05	3.600e-14	6.500e-01	3.732e-03	5.220e+01	1.081e-02	6.500e-08	1.350e+00	2.055e-04
7.500e+05	3.500e-14	6.600e-01	3.934e-03	5.300e+01	1.218e-02	6.600e-08	1.340e+00	2.087e-04
7.600e+05	3.400e-14	6.700e-01	4.146e-03	5.380e+01	1.374e-02	6.700e-08	1.330e+00	2.118e-04
7.700e+05	3.300e-14	6.800e-01	4.369e-03	5.460e+01	1.549e-02	6.800e-08	1.320e+00	2.150e-04
7.800e+05	3.200e-14	6.900e-01	4.604e-03	5.540e+01	1.747e-02	6.900e-08	1.310e+00	2.181e-04
7.900e+05	3.100e-14	7.000e-01	4.851e-03	5.620e+01	1.972e-02	7.000e-08	1.300e+00	2.213e-04
8.000e+05	3.000e-14	7.100e-01	5.111e-03	5.700e+01	2.226e-02	7.100e-08	1.290e+00	2.245e-04
8.100e+05	2.900e-14	7.200e-01	5.385e-03	5.780e+01	2.514e-02	7.200e-08	1.280e+00	2.276e-04
8.200e+05	2.800e-14	7.300e-01	5.675e-03	5.860e+01	2.841e-02	7.300e-08	1.270e+00	2.308e-04
8.300e+05	2.700e-14	7.400e-01	5.981e-03	5.940e+01	3.213e-02	7.400e-08	1.260e+00	2.340e-04
8.400e+05	2.600e-14	7.500e-01	6.305e-03	6.020e+01	3.636e-02	7.500e-08	1.250e+00	2.371e-04
8.500e+05	2.500e-14	7.600e-01	6.648e-03	6.100e+01	4.120e-02	7.600e-08	1.240e+00	2.403e-04
8.600e+05	2.400e-14	7.700e-01	7.013e-03	6.180e+01	4.673e-02	7.700e-08	1.230e+00	2.434e-04
8.700e+05	2.300e-14	7.800e-01	7.401e-03	6.260e+01	5.308e-02	7.800e-08	1.220e+00	2.466e-04
8.800e+05	2.200e-14	7.900e-01	7.814e-03	6.340e+01	6.038e-02	7.900e-08	1.210e+00	2.498e-04
8.900e+05	2.100e-14	8.000e-01	8.255e-03	6.420e+01	6.879e-02	8.000e-08	1.200e+00	2.529e-04
9.000e+05	2.000e-14	8.100e-01	8.727e-03	6.500e+01	7.852e-02	8.100e-08	1.190e+00	2.561e-04
9.100e+05	1.900e-14	8.200e-01	9.235e-03	6.580e+01	8.982e-02	8.200e-08	1.180e+00	2.593e-04
9.200e+05	1.800e-14	8.300e-01	9.781e-03	6.660e+01	1.030e-01	8.300e-08	1.170e+00	2.624e-04
9.300e+05	1.700e-14	8.400e-01	1.037e-02	6.740e+01	1.184e-01	8.400e-08	1.160e+00	2.656e-04
9.400e+05	1.600e-14	8.500e-01	1.101e-02	6.820e+01	1.366e-01	8.500e-08	1.150e+00	2.687e-04
9.500e+05	1.500e-14	8.600e-01	1.171e-02	6.900e+01	1.581e-01	8.600e-08	1.140e+00	2.719e-04
9.600e+05	1.400e-14	8.700e-01	1.248e-02	6.980e+01	1.839e-01	8.700e-08	1.130e+00	2.751e-04
9.700e+05	1.300e-14	8.800e-01	1.333e-02	7.060e+01	2.148e-01	8.800e-08	1.120e+00	2.782e-04
9.800e+05	1.200e-14	8.900e-01	1.427e-02	7.140e+01	2.524e-01	8.900e-08	1.110e+00	2.814e-04
9.900e+05	1.100e-14	9.000e-01	1.533e-02	7.220e+01	2.986e-01	9.000e-08	1.100e+00	2.846e-04
1.000e+06	1.000e-14	9.100e-01	1.653e-02	7.300e+01	3.561e-01	9.100e-08	1.090e+00	2.877e-04
1.010e+06	9.000e-15	9.200e-01	1.790e-02	7.380e+01	4.288e-01	9.200e-08	1.080e+00	2.909e-04
1.020e+06	8.000e-15	9.300e-01	1.951e-02	7.460e+01	5.229e-01	9.300e-08	1.070e+00	2.940e-04
1.030e+06	7.000e-15	9.400e-01	2.142e-02	7.540e+01	6.475e-01	9.400e-08	1.060e+00	2.972e-04
1.040e+06	6.000e-15	9.500e-01	2.376e-02	7.620e+01	8.185e-01	9.500e-08	1.050e+00	3.004e-04
1.050e+06	5.000e-15	9.600e-01	2.672e-02	7.700e+01	1.064e+00	9.600e-08	1.040e+00	3.035e-04
1.060e+06	4.000e-15	9.700e-01	3.065e-02	7.780e+01	1.440e+00	9.700e-08	1.030e+00	3.067e-04
1.070e+06	3.000e-15	9.800e-01	3.631e-02	7.860e+01	2.081e+00	9.800e-08	1.020e+00	3.099e-04
1.080e+06	2.000e-15	9.900e-01	4.562e-02	7.940e+01	3.380e+00	9.900e-08	1.010e+00	3.130e-04
1.090e+06	1.000e-15	1.000e+00	6.615e-02	8.020e+01	7.323e+00	1.000e-07	1.000e+00	3.162e-04

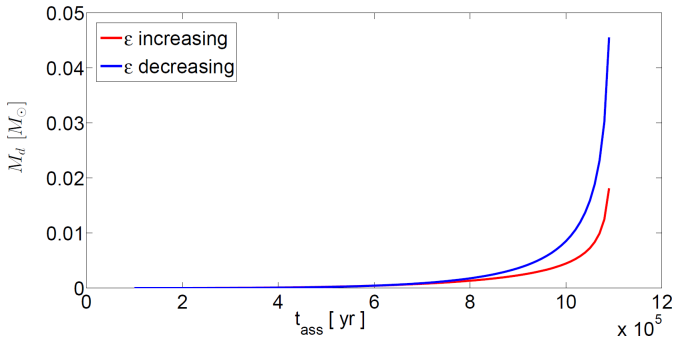

Figure 1. *Disk crossing or assembly time versus disk mass. The red curve represents when $\epsilon = L_{rad}/L_{gf}$ of the initially collapsing cloud core decreases, and the blue curve represents when ϵ increases. Assuming $R_\star \approx R_\odot$, c_{sR}= 330-300 ms^{-1} & c_{sr}= 220-200 ms^{-1}.*

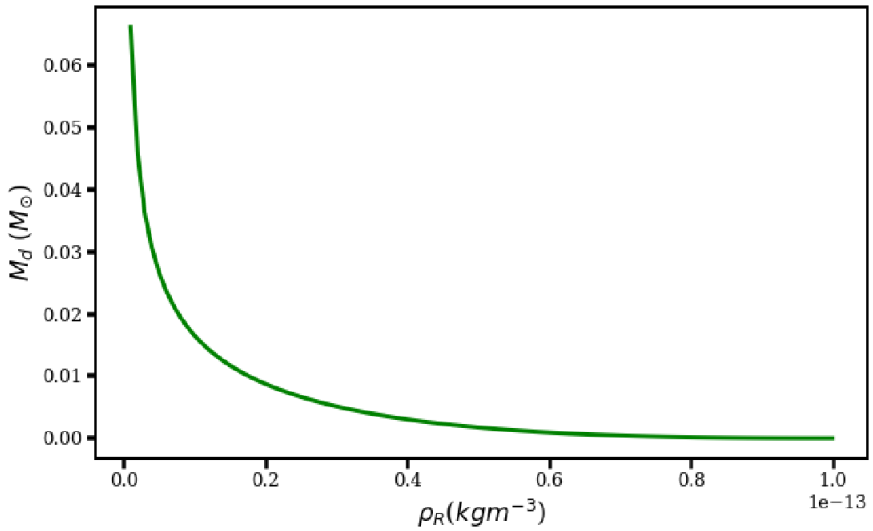

Figure 2. *The envelope density in relation to disk mass When the envelope temperature is increasing from 10-19.9K, T_r = 1000-10999K, ϵ raising from 0.099-0.99, $t_{ass} = 10^5 - 10^{6.4}$ yr, $R_\star \approx R_\odot$ and other parameters are as indicated in the boundary condition mentioned under section 3.6. Note that we have been using R instead of R_c in some places to avoid double subscript. Thus, the terms $\rho_R = \rho_{Rc} = \rho_c$ are interchangeable.*

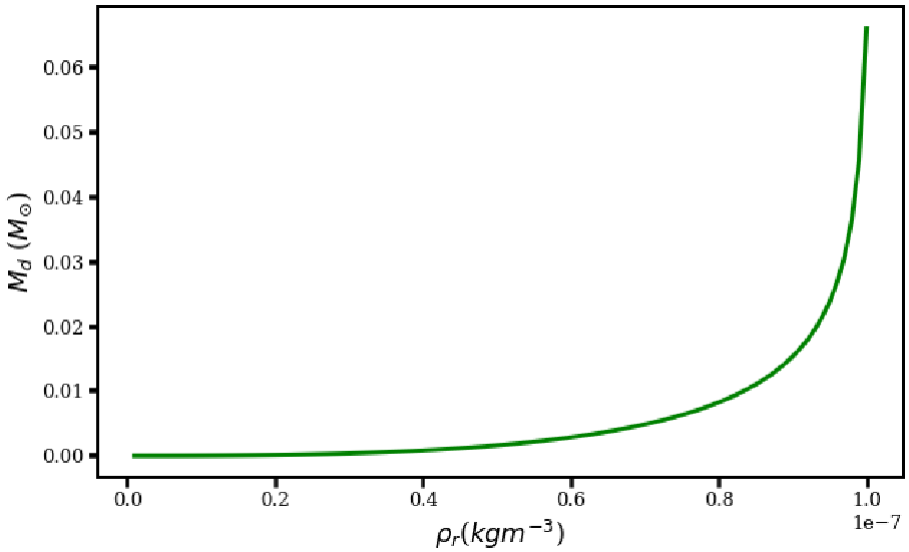

Figure 3. *Density of central core vs protoplanetary disc mass. Assuming increasing ϵ= 0.099-0.99, cloud core radius R = 0.01 - 1pc, temperature T_c = 10 -19.9K, $\rho_c = 10^{-13} - 10^{-15} kgm^{-3}$ reducing with increasing radius, central core temperature T_{core} = 1000 - 10999K, density $\rho_{core} = 10^{-9} - 10^{-7} kgm^{-3}$, disk radius R_d = 1- 80.5AU, sound speed in the envelope c_{sR}= 300 - 329.9 ms^{-1}, sound speed in central core c_{sr} = 219.9 - 200 ms^{-1}, central core radius r_{core} = 1.99 - 1$R_\odot$ and $\Omega_\star = 10^{-5.5} - 10^{-3.5} s^{-1}$. Here, we consider that the central core forms a hosting star in time. from 1.*

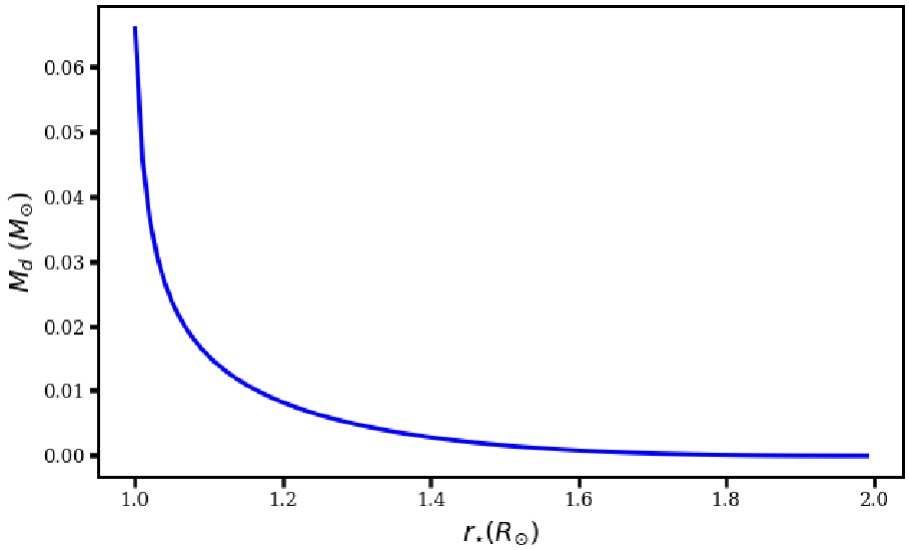

Figure 4. *The host star radius vs. protoplanetary disk mass. Assuming R_c= 0.01 - 1pc, T_c = 10 - 19.9K, e= 0.099-0.99, $c_R \approx 329 - 300ms^{-1}$, $c_r \approx 219 - 200ms^{-1}$, $\Omega_\star \sim 10^{-4.5}s^{-1}$, $T_r \sim$ 1000-10999K, $t \sim 10^5 yr$, R_d 1 - 50.5AU, $\rho_c = 10^{-13} - 10^{-15}kgm^{-3}$, $\rho_r = 10^{-9} - 10^{-7}kgm^{-3}$ and other parameters are supposed to vary as mentioned under Section 3.6. The graph shows the disk mass and the hosting star mass are governed by complex physical processes and parameters. There is no single best parameter to describe the disk formation, but the combination of many parameters fixes the mass.*

Figure 3 tells us that the larger the radius of the host star, the minimum the disk mass is. As the radius of the central stellar object becomes larger, the object will become luminous and reduce the rate of matter accumulating in the disk. Figure 2 indicates that as the envelope becomes denser and other parameters increase, the forming disk mass reduces. The interplay between thermodynamic factors (ϵ), core temperature, and the envelope density governs the rate of disk mass growth.

3.7. Disk Formation in a Magnetized Cloud

3.7.1. Disk Mass

If the disk forms in a strongly magnetized cloud, the flux traversing the disk is$\Phi_d = \pi R_d^2 B_d$, whereas the flux traversing the cloud core is $\Phi_c = \pi R_c^2 B_c$. We get $\Phi_d = \Phi_c$, from the flux conservation, which implies$\pi R_d^2 B_d = \pi R_c^2 B_c$ when we apply this conservation concept and multiply Eqn.(19) by $\frac{\Phi_c}{\Phi_c}$.

$$M_{md}(t_{ass}) \approx 1.1 \times 10^{-3} \left[\frac{1}{\rho_c c_{sR}^2}\right]^{1/2} \left[\frac{T_c^{7/2}}{\epsilon^2 R_c^6}\right]^{1/5} \times \frac{\rho_{(r)} c_{sr}^2}{T_r} R_d^5 \frac{\pi B_d}{\Phi_c}\, t_{ass} \tag{37}$$

Finally, M_{md} is mass of magnetized disk.

$$M_{dm}(t_{ass}) \approx 1.1 \times 10^{-3} \left[\frac{1}{\rho_c c_{sR}^2}\right]^{1/2} \left[\frac{T_c^{7/2}}{\epsilon^2 R_c^{16}}\right]^{1/5} \times \frac{\rho_{(r)} c_{sr}^2}{T_r} \frac{R_d^5\, B_d}{B_c}\, t_{ass} \tag{38}$$

where B_c and B_d are the cloud core and the disk magnetic field respectively.

3.7.2. Density

The density of the magnetized disk can be obtained by taking into account the spherical disk from Eqn. (25)

$$\rho_{dm}(t_{ass}) \approx 2.63 \times 10^{-4} \left[\frac{1}{\rho_c c_{sR}^2}\right]^{1/2} \left[\frac{T_c^{7/2}}{\epsilon^2 R_c^{16}}\right]^{1/5} \times \frac{\rho_{(r)} c_{sr}^2}{T_r} \frac{R_d^2\, B_d}{B_c}\, t_{ass} \tag{39}$$

where ρ_{md} is density of magnetized disk.

3.7.3. Angular Momentum

Substituting Eqn.(38) Instead of disk mass in Eqn.(34) we get momentum carried by the magnetized disk.

$$J_d = 2.63 \times 10^{-4} \left(G M_\star R_d^{11}\right)^{1/2} \left[\frac{1}{\rho_c c_{sR}^2}\right]^{1/2} \left[\frac{T_c^{7/2}}{\epsilon^2 R_c^{16}}\right]^{1/5} \times \frac{\rho_{(r)} c_{sr}^2}{T_r} \frac{B_d}{B_c}\, t_{ass} \tag{40}$$

this indicates $J_d \propto R_d^{11/2}$, $J_d \propto B_d$, $J_d \propto B_{core}^{-1}$. If the magnetic flux of the central core and the initial cloud is the same by conservation law $\Phi_{core} = \Phi_c$.

3.7.4. Disk and Stellar Mass Relation

Now, using Eqn. (38) in Eqn. (35) the disk stellar mass relation for a magnetized system is described as

$$M_\star = G\frac{R_d\left[1.1\times10^{-3}\left[\frac{1}{\rho_c c_{sR}^2}\right]^{1/2}\left[\frac{T_c^{7/2}}{\epsilon^2 R_c^{16}}\right]^{1/5}\frac{\rho_{(r)}c_{sr}^2}{T_r}\frac{R_d^5 B_d}{B_c}\,t_{ass}\right]^2}{\Omega_\star^2 R_\star^4} \tag{41}$$

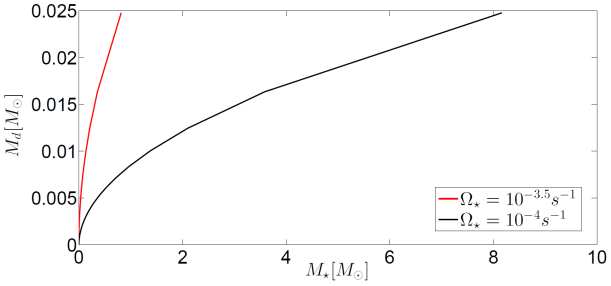

Figure 5. *Host star mass vs its protoplanetary disk mas. With parameters range ϵ= 0.9, R_c = 0.01pc, T_c = 10K, $\rho_c = 10^{-13} - 10^{-15}kgm^{-3}$, T_{core} = 5000K, $\rho_{core} = 10^{-9} - 10^{-7}kgm^{-3}$, R_d = 1- 100AU, c_{sR}= 300 - 332 ms^{-1}, c_{sr} = 200 ms^{-1}, r_{core} = 1 - 1.99$R_\odot$, $t_{ass} = 10^{-5}yr$, $t_{ass} = 10^5 - 10^{6.04}yr$, $B_c = 1G$ and $B_d = 10^{-1}G$. Here, we consider that the central core forms a hosting star in time. Plotted from Eqn. (38).*

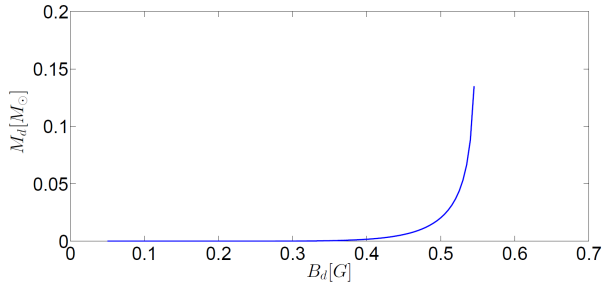

Figure 6. *The disk magnetic field vs. protoplanetary disk mass with various parameter ranges ϵ= 0.9, R_c = 0.01pc, T_c = 10K, $\rho_c = 10^{-13} - 10^{-15}kgm^{-3}$, T_{core} = 5000K, $\rho_{core} = 10^{-9} - 10^{-7}kgm^{-3}$, R_d = 1- 100AU, c_{sR}= 300 - 332 ms^{-1}, c_{sr} = 200 ms^{-1}, r_{core} = 1 - 1.99$R_\odot$, $t_{ass} = 10^{-5}yr$, $t_{ass} = 10^5 - 10^{6.04}yr$, $B_c = 1G$ and $\Omega_\star = 10^{-3.5}s^{-1}$. Plotted from Eqn. (38).*

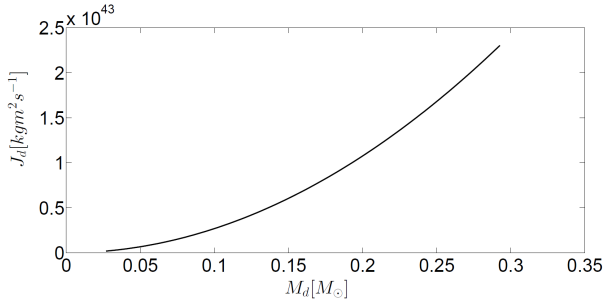

Figure 7. *Protoplanetary disk mass vrs Its total angular momentum. From parameters range ϵ= 0.9, R_c = 0.01pc, T_c = 10K, $\rho_c = 10^{-13}kgm^{-3}$, T_{core} = 5000K, $\rho_{core} = 10^{-7}kgm^{-3}$, R_d = 50AU, c_{sR}= 332 ms^{-1}, c_{sr} = 200 ms^{-1}, r_{core} = 1$R_\odot$, $t_{ass} = 10^{5.5}yr$, $B_c = 10^{-4}G$ and $\Omega_\star = 10^{-3}s^{-1}$. Plotted from Eqn. (40).*

The magnetic field at an average place on the Sun is around 1 Gauss, about twice as strong as the average field on the surface of Earth (around 0.5 Gauss). Protoplanetary disk had a magnetic field intensity between 0.05 and 0.5 gauss. The Sun like star has a break-up angular velocity $\Omega_b \sim 10^{-3}s^{-1}$ (corresponding to a few hundred km/s).

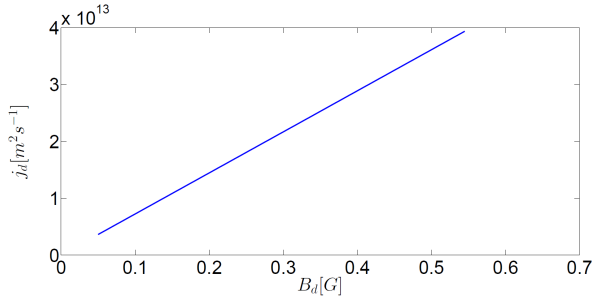

Figure 8. *The magnetic field of the disk vs The protoplanetary disk specific angular momentum. Range of parameters ϵ= 0.9, R_c = 0.01pc, T_c = 10K, $\rho_c = 10^{-13}kgm^{-3}$, T_{core} = 5000K, $\rho_{core} = 10^{-7}kgm^{-3}$, R_d = 50AU, c_{sR}= 332 ms^{-1}, c_{sr} = 200 ms^{-1}, r_{core} = 1$R_\odot$, $t_{ass} = 10^{5.5}yr$, $B_c = 10^{-4}G$ and $\Omega_\star = 10^{-3}s^{-1}$. Plotted from Eqn. (40).*

4. Discussion

The results show that the protoplanetary disk properties can be expressed in terms of the parent MC core (prestellar core) properties. Figure 1 indicates the rise in the central core temperature reduces the disk's mass. This leads to the decrement of the disk's mass because the high temperature at the middle of the disk causes dispersion of the disk's gas. Figures 1 to 4 indicate the relationship between the disk, parent cloud, and the host star properties. Figures 5 to 8 indicate how the magnetic field influences the disk mass growth in time. In addition, the momentum transport is also affected by the magnetic field strength of the parent cloud or the central core as well as of the disk.

The disk's temperature is explained in different ways at the early formation time and the late formation time. At the very early formation time (at $t_{ass} \ll 1$ million years), the disk temperature is independent of its radius since r = R_d. Whereas in the late disk assembly time, its temperature is $T_{psd} \propto R_d^{-3/4}$ provided that r $\neq R_d$. These temperature profiles mainly work when accretion is the dominant source of energy. After accretion ceases, the source of energy will be either irradiation or another process, and the equation of temperature may change.

5. Conclusions

Current protoplanetary disk formation models explain a wide variety of complex observed data, but remain incomplete.

In this work, we have argued that the properties of the pre-stellar core directly influence how the resulting planetary disk will look. The physical mechanisms related to the protoplanetary disk formation process are very complex. Despite all this uncertainty, we theoretically model the relationship between some fundamental disk properties and the cloud core from which they originate. The model shows the process depends strongly on the amount of raw material available in the parent cloud core. In this study, we have shown that the properties of protostellar and protoplanetary disk formation mainly depend on the properties of their parent cloud core.

The observation of the protoplanetary disk presents challenges due to its small size, low mass, and cool temperatures. To overcome these challenges, we have developed theoretical models that describe the equations for disk mass, density, and temperature in relation to the parent cloud core, also known as the pre-stellar core. In this paper, we have established the relationship between the properties of the disk and the properties of the parent MC core. The temperature of the disk is explained in two different ways: one for early disk formation and another for late disk formation. This allows us to understand the role of disk assembly time. Additionally, we have formulated how density and temperature change over time during the disk formation process. When matter accretion stops during disk formation, we need to derive a new theoretical formula for temperature and density, as the disk may dissipate or evolve into a planetary system without mass infall. However, the density may remain constant once stars and planets have fully formed in a given system. Furthermore, we have demonstrated how mass-momentum transfer influences the mass of the disk and the host star.

We have demonstrated that the disk mass (M_d) is related to various factors. Firstly, it is proportional to the temperature of the core (T_c) raised to the power of 7/10. Secondly, it is inversely proportional to the temperature of the parent molecular cloud (T_r). Thirdly, it is proportional to the radius of the cloud (R) raised to the power of -6/5. Additionally, the disk mass is proportional to the assembly time (t_{ass}) and the radius of the disk (r) raised to the power of 3.

As a result of these relationships, we can conclude that the disk mass is inversely proportional to the turbulence pressure in the parent molecular cloud (P_R) raised to the power of -1/2, and directly proportional to the turbulence in the core (P_r). Furthermore, when the disk formation occurs in a strongly magnetized cloud, the mass of the magnetized disk is proportional to the inverse of the product of the radius of the core (R_c) raised to the power of -16/5, the radius of the disk (R_d) raised to the power of 5, the magnetic field of the disk (B_d), and the inverse of the magnetic field of the core (B_c). Similarly, the density of the magnetized disk is proportional to the inverse of the product of R_c raised to the power of -16/5, R_d raised to the power of 2, B_d, and the inverse of B_c. The total angular momentum is proportional to the product of B_d and the inverse of B_c.

The mass-momentum transfer method has been utilized to establish the relationship between the mass of the parent molecular cloud or envelope, the protoplanetary disk, and the mass of the host star. We have found that the mass of the host star is proportional to the product of R_d raised to the power of 5/2, B_d raised to the power of 2, and the inverse of B_c for the magnetized cloud and disk. These models will enable us to determine the type of molecular cloud core from which currently evolving stars and planetary systems are formed, as well as predict the type of protoplanetary disk that will form from the evolving molecular cloud.

Acknowledgments

We express our sincere gratitude to the Space Science and Geospatial Institute (SSGI), Entoto Observatory and Research Center (EORC), Department of Astronomy and Astrophysics, and International Science Programme (ISP)-Uppsala University through the East African Astrophysics Research Network (EAARN) for their invaluable support in facilitating this study. Additionally, we would like to acknowledge Jimma University for their support in enabling Gemechu Muleta Kumssa to conduct this research.

Conflicts of Interest

All the authors do not have any possible conflicts of interest.

References

[1] ALMA Partnership, Vlahakis, C., Hunter, T. R. et al. 2015, July, ApJ, 808 (1), L4.

[2] Ansdell M. et al., 2016, ApJ, 828, 46.

[3] Anathpindika, S., & di Francesco, J. 2013, April, MNRAS, 430 (3), 1854-1866.

[4] Armitage, P. J. 2010, Astrophysics of Planet Formation.

[5] Bohlin, R. C., Savage, B. D., & Drake, J. F. 1978, August, ApJ, 224, 132-142.

[6] Calvet, N., Hartmann, L., & Strom, S. E. 2000, Protostars and Planets IV, 377.

[7] Ward-Thompson, D., & Whitworth, A. P. 2011, An Introduction to StarFormation.

[8] Cox, E. G., Harris, R. J., Looney, L. W. et al. 2017, December, ApJ, 851 (2), 83.

[9] Elmegreen, B. G., & Scalo, J. 2004, ARAA, 42, 211.

[10] Enoch, M. L., Corder, S., Dunham, M. M., & Duch?ne, G. 2009, December, ApJ, 707 (1), 103-113.

[11] Kumssa, G. M. and Tessema, S. B., 2019, Astronomische Nachrichten, 340 (8), pp. 736-743.

[12] Rosotti et al., 2017, MNRAS, 468 (2): 1631-8.

[13] Hartmann et al., 2005, Astronomy and Astrophysics, 440 (2), pp. 775-782.

[14] Hildebrand, R. H. 1983, QJRAS, 24, 267.

[15] Jonathan P. Williams and Lucas A. Cieza, 2011, 10.1146/annurev-astro-081710-102548.

[16] R. S. Klessen and P. Hennebelle, 2010, AA 520, A17 (2010).

[17] Kennicutt Jr, R. C. and Evans, N. J., 2012, Annual Review of Astronomyand Astrophysics, 50, pp. 531-608.

[18] Kenyon, S. J., and Bromley, B. C. 2009, September, VizieR Online DataCatalog, J/ApJS/179/451.

[19] Kolb, U., 2010, Extreme environment astrophysics. Cambridge UniversityPress, pp. 11-12.

[20] Lee, N., Williams, J. P. and Cieza, L. A., 2011, ApJ, 736 (2), p. 135.

[21] Mac Low, M. M. and Klessen, R. S., 2004, Reviews of modern physics, 76 (1), p. 125.

[22] McKee, C. F. and Ostriker, E. C., 2007, Annu. Rev. Astron. Astrophys., 45, pp. 565-687.

[23] Mann, R. K., Di Francesco, J., Johnstone, D. et al. 2014, March, ApJ, 784 (1), 82.

[24] Mann, R. K., Andrews, S. M., Eisner, J. A., Williams, J. P., Meyer, M. R., Di Francesco, J., Carpenter, J. M. and Johnstone, D., 2015. Protoplanetarydisk masses in the young NGC 2024 cluster. The Astrophysical Journal, 802 (2), p. 77.

[25] Matsumoto, T., and Hanawa, T. 2003, October, ApJ, 595 (2), 913-934.

[26] Najita et al., 2015, MNRAS, 450 (4), 3559-3567.

[27] Nixon et al., 2018, July, MNRAS, 477 (3), 3273-3278.

[28] Okuzumi et al., ApJ, 821 (2), p. 82.

[29] Palla, F., 2002, Physics of Star Formation in Galaxies (pp. 9-133). Springer, Berlin, Heidelberg.

[30] Robitaille, T. P., Whitney, B. A., Indebetouw, R., Wood, K. and Denzmore, P., 2006. Interpreting spectral energy distributions from young stellar objects. I. A grid of 200,000 YSO model SEDs. The Astrophysical Journal Supplement Series, 167 (2), p. 256.

[31] Seifried et al., 2013 MNRAS, 432 (4), pp. 3320-3331.

[32] Walch et al., 2010, MNRAS, 402 (4), 2253-2263.

[33] Williams, J. P., and Best, W. M. J. 2014, ApJ, 788, 59.

[34] Williams J. P., Cieza L. A., 2011, ARA and A, 49, 67.

[35] Walch et al., 2017, MNRAS, 467 (1), pp. 922-927.